Journal Pre-proofs

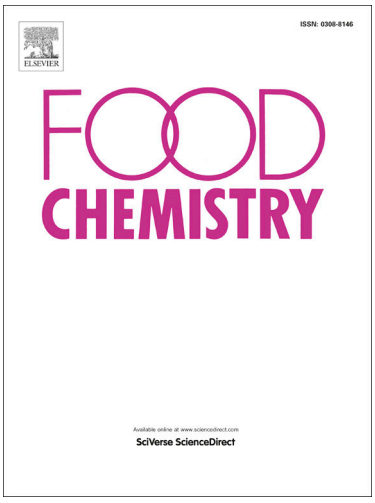

Effects of three processing technologies on the structure and immunoreactivity of α-tropomyosin from *Haliotis discus hannai*

Nairu Ji, Chenchen Yu, Xinyu Han, Xinrong He, Shuai Kang, Tianliang Bai, Hong Liu, Guixia Chen, Minjie Cao, Guangming Liu

PII: S0308-8146(22)02909-0
DOI: https://doi.org/10.1016/j.foodchem.2022.134947
Reference: FOCH 134947

To appear in: *Food Chemistry*

Received Date: 12 August 2022
Revised Date: 9 November 2022
Accepted Date: 10 November 2022

Please cite this article as: Ji, N., Yu, C., Han, X., He, X., Kang, S., Bai, T., Liu, H., Chen, G., Cao, M., Liu, G., Effects of three processing technologies on the structure and immunoreactivity of α-tropomyosin from *Haliotis discus hannai*, *Food Chemistry* (2022), doi: https://doi.org/10.1016/j.foodchem.2022.134947

Effects of three processing technologies on the structure and immunoreactivity of α-tropomyosin from *Haliotis discus hannai*

Nairu Ji[1], Chenchen Yu[1], Xinyu Han[1], Xinrong He[1], Shuai Kang[1], Tianliang Bai[1], Hong Liu[1], Guixia Chen[2], Minjie Cao[1], Guangming Liu[1]*

[1] *College of Ocean Food and Biological Engineering, Xiamen Key Laboratory of Marine Functional Food, Fujian Provincial Engineering Technology Research Center of Marine Functional Food, Jimei University, Xiamen, Fujian 361021, China*

[2] *Women and Children's Hospital Affiliated to Xiamen University, Xiamen, Fujian 361003, China*

Running title: Effect on immunoreactivity of tropomyosin from abalone after three technologies

Corresponding author:

*Guang-Ming Liu,

College of Ocean Food and Biological Engineering, Jimei University

Phone: +86-592-6183383

Fax: +86-592-6180470

Email: gmliu@jmu.edu.cn

Abbreviations

Arab, arabinose**;** **BSA**, bovine serum albumin; **ELISA**, enzyme-linked immunosorbent assay; **Fru**, fructose; **Gal**, galactose; **GlcN**, glucosamine; **Glu**, glucose; **Ig**, Immunoglobulin; **MW**, molecular weight; **OD**, optical density; **SDS-PAGE**,

22 sodium dodecyl sulfate polyacrylamide gel electrophoresis; **TG**, transglutaminase; **TM**,

23 tropomyosin; **Xyl**, xylose; **3D**, three-dimensional; **α-TM**, subunit of TM; **α_2-TM**,

24 supercoil of TM; **α-TMT**, TG-catalyzed cross-linking reaction with α-TM; **α-TMGT**,

25 TG-catalyzed glycosylation with α-TM; **α-TMX**, glycation with α-TM and xylose.

Abstract

The subunit of tropomyosin (α-TM) from *Haliotis discus hannai* is an important allergen. The methods to reduce the immunoreactivity of α-TM are worth investigating. Thus, this study confirmed the reacted conditions of α-TM with transglutaminase (TG)-catalyzed cross-linking reaction, TG-catalyzed glycosylation, and glycation. Three processing technologies reduced significantly the contents of α-helix and hydrophobic force of α-TM and increased the surface hydrophobicity. A serological experiment confirmed that the glycated α-TM with xylose showed the lowest IgG/IgE-binding capacity. The inhabitation dot blot displayed that five epitope peptides could bind with the site-specific IgE prepared by the glycated α-TM. Three in nine glycated sites (M68, N202, and N203) were verified to modify two epitopes (L-HTM-3 and L-HTM-7) of α-TM, which affected the immunoreactivity of α-TM during glycation. These results indicated that glycation would be desired for developing hypo-allergenic abalone products.

Key words: Epitope peptides; *Haliotis discus hannai*; Immunoreactivity; Processing technologies; Structure of α-helix; Tropomyosin

1 Introduction

Shellfish allergy is a typical reaction mediated by Immunoglobulin (Ig) E (Anvari, Miller, Yeh, & Davis, 2019). Shellfish allergy could lead to adverse immune responses in respiratory, digestive, and nervous systems (Ho, Wong, & Chang, 2014). As a pan-allergen, tropomyosin (TM) displayed the coiled-coil structure composed by two subunits (Costa et al 2022), presenting a molecular weight (MW) around 34-38 kDa (Faber et al., 2017). TM has been identified in both crustaceans (crab, prawn, lobster) and molluscans (oyster, snail, abalone, squid) (Suh, Kim, Kim, Kim, & Kim, 2020; Costa et al., 2022). Recently, the subunit of TM (α-TM) and supercoil of TM (α_2-TM) were identified from *Haliotis discus hannai* (Ji et al., 2021). However, there is no efficient approach to eliminate or reduce its immunoreactivity.

Most studies focused on processing the purified TM, which is easier to explore the reason for the change in immunoreactivity. However, traditional approaches are hard to reduce allergenicity, like boiling, frying, and freezing (Faisal, Vasiljevic, & Donkor, 2018; Liu et al., 2021). α-TM was more heat-resistant than α_2-TM (Ji et al., 2021). Thus, the hypo-immunoreactivity by processing with the purified α-TM from *H. discus hannai* is worthy of study. There are many processing technologies to change the immunoreactivity of TM. Tyrosinase/caffeic acid, laccase/caffeic acid, transglutaminase (TG) cross-linking, TG-catalyzed glycosylation, and glycation could decrease the IgG/IgE-binding capacity of shrimp TM (Ahmed et al., 2020; Ahmed et al., 2021; Yuan, Lv, Li, Mi, Chen, & Lin, 2016; Zhang, Li, Xiao, Nowak-Wegrzyn, & Zhou, 2020). The above processing methods might be potent approaches to change the allergenicity of TM from abalone.

The secondary structure of TM consisted of α-helix. Many studies had shown that the antigenicity of TM was reduced after processing when the content of α-helix was

decreased (Yuan, Lv, Li, Mi, Chen, & Lin, 2016; Zhang, Xiao, Zhang, & Zhou, 2018). The structure of TM was unfolded after high hydrostatic pressure (Jin, Deng, Qian, Zhang, Liu, & Zhao, 2015). The hydrophobicity of crab TM was increased by the glycation with arabinose (Han, et al., 2018). The absolute value of the zeta potential is 25-30 mV, which is the threshold for the stability of the protein solution (Thaiphanit, Schleining, & Anprung, 2016). However, the structure changes of α-TM after processing are still unknown. The relationship between the structure and immunoreactivity of α-TM is also needed to explore.

An antigenic epitope is a basis for activating the individual's immune system and resulting in the allergy (Liu, & Sathe, 2018). Xi & He (2020) found the destroyed epitopes of Gly m Bd 60 K by the site-specific IgG and phage display technology. The higher frequency of amino acids (Lysine, Proline, Glycine, Alanine, and Threonine) on epitopes are responsible for the bends or flexibility in the epitope region, which is related to the allergenicity (Yang et al., 2019). Han et al. (2018) and Bai et al. (2021) found that the allergenicity of TM from crab and scallop was decreased after glycation. The modified sites (Arginine and Lysine) were located on the epitopes of TM, which indicated that alternation of epitopes was related to allergenicity during glycation (Han et al., 2018; Bai et al., 2021). The affected epitopes and the modified amino acids of the processed α-TM will be the focus.

Thus, this work aimed to explain the effects of the TG-catalyzed cross-linking reaction, TG-catalyzed glycosylation, and glycation on the immunoreactivity of α-TM in *H. discus hannai*. α-TM was purified to prepare three processed products. The structure, IgG/IgE-binding capacity, and identification of modified sites would characterize the effects on α-TM after the TG-catalyzed cross-linking reaction, TG-

92 catalyzed glycosylation, and glycation. This study might provide a new perspective on
93 the desensitization of *H. discus hannai*-induced allergy.

94 **2 Material and methods**

95 **2.1 Materials**

96 Live *H. discus hannai* were purchased from Jimei Market (Xiamen, Fujian, China)
97 and sacrificed immediately. The TG, glucose (Glu), fructose (Fru), arabinose (Arab),
98 xylose (Xyl), and galactose (Gal) were purchased from Macklin (Shanghai, China). The
99 glucosamine (GlcN) was purchased from Sigma-Aldrich (St Louis, Missouri, USA).
100 The rabbit anti-*H. discus hannai* TM polyclonal antibody was prepared in our
101 laboratory before (Ji et al., 2021). Horseradish peroxidase-labeled goat anti-human IgE
102 antibody and horseradish peroxidase-labeled anti-rabbit IgG antibody was purchased
103 from Southern Biotech (Birmingham, Alabama, USA).

104 **2.2 Human sera**

105 Sera were obtained from the Women and Children's Hospital Affiliated to Xiamen
106 University (human ethical approval No. KY-2019-014, Xiamen, Fujian, China). The
107 abalone-sensitized patients were selected based on both a positive IgE test ($f_{22} \geq 0.35$
108 kU/L) to shrimp extracts and their clinical history related to abalone. The optical density
109 (OD) at 450 nm ≥ 0.10 to α-TM was defined as positive (Table 1) by enzyme-linked
110 immunosorbent assay (ELISA). Signed informed consent was obtained from all
111 individuals. Sera from 10 abalone-sensitized patients and 2 healthy people (No. 1 ~ 12)
112 were stored at -80 °C until further use.

113 **2.3 Preparation of α-TM and three processed products**

The *H. discus hannai* was slaughtered with a knife to remove the shell. The muscle was sliced to purify α-TM according to the previous method by Ji et al. (2021). Then, α-TM was treated by TG-catalyzed cross-linking, TG-catalyzed glycosylation, and glycation as previously reported with some modifications (Ahmed et al., 2021; Yuan, Lv, Li, Mi, Chen, & Lin, 2016; Bai et al., 2021). The steps of purification of α-TM and optimization of the three processing technologies were shown in "Method" section of Supporting Information.

All the products were analyzed by sodium dodecyl sulfate polyacrylamide gel electrophoresis (SDS-PAGE), Western blot, average particle size, and zeta potential. The average particle size and zeta potential were measured using the Zetasizer Nano Series Nano-ZS (Malvern Instruments Ltd, Malvern, Worcestershire, UK) and analyzed by Malvern Mastersizer software according to the method of Liu et al. (2019). The sample was scanned 20 times in once, and repeated thirdly.

2.4 Comparison of the structure of α-TM and its processed products

The secondary structure and surface hydrophobicity of α-TM and three processed products were analyzed (Bai et al., 2021). Briefly, the secondary structure f α-TM and its processed products were measured using the Circular Dichroism spectrum (Applied Photophysics, Ltd., Surrey, UK) and calculated by CDNN software. The measurement of chemical bonds was performed according to Ji et al. (2021) to calculate the contents of the ionic bond, hydrogen bond, hydrophobic force, and disulfide bond.

The UV absorption spectra are according to the method of Liu et al. (2021) with some modifications. α-TM and three processed products were adjusted to 0.2 mg/mL

to measure the absorbance at 200-500 nm. The absorbance at 294 nm, 320 nm, and 420 nm was used to analyze the degree of glycation. The type of glycan bond of α-TM after processing was analyzed by Ruan et al. (2013). The processed products were treated with NaOH for 16 h to measure the absorbance at 200-300 nm, and the processed products without NaOH were control groups.

2.5 Comparison of the immunoreactivity of α-TM and its processed products

The specific IgG/IgE-binding capacity of α-TM and three processed products were detected as described by Shen et al. (2012). The rabbit anti-*H. discus hannai* TM polyclonal antibody (1:1×10^6 dilution) and abalone-sensitized patients' sera (1:3 dilution) was used as the primary antibody, respectively.

Furthermore, an inhibition ELISA was analyzed according to the method (Ji et al., 2021). α-TM was incubated at the solid plate; α-TM or its processed products was diluted into different concentrations to preincubate with the rabbit anti-*H. discus hannai* TM polyclonal antibody.

2.6 Preparation of site-specific IgE and analysis of the ability to recognize epitope peptides

The preparation procedure was according to the method of Xi & He (2020) with slight modifications. An excess of processed (TG-catalyzed cross-linking, TG-catalyzed glycosylation, and glycation) α-TM was added to the abalone-sensitized sera pool to incubate at 4 °C overnight, and centrifugated (10000 *g*, 30 min, 4 °C) to remove the precipitation. Then, the identified epitopes from Ji et al. (2021) were listed in Supporting Information Table S2. The corresponding peptides were added to the

supernatant as the primary antibody in the inhibition dot blot.

2.7 Identification of the modified sites of α-TM after glycation

The modified sites of the glycated α-TM were analyzed at Shanghai Bioprofile Technology Company Ltd. Firstly, the glycated α-TM was hydrolyzed with trypsin and then desalted by a C18 column, and then freeze-dried. The freeze-dried sample was dissolved with Lectin mixture for 1 h and centrifugated (14000 *g*, 30 min, 4 °C). Then, the sample was digested by PNGase F overnight at 37 °C and collected to lyophilize again. The lyophilized sample was separated using the Easy nLC 1200 chromatographic system (Thermo Scientific, Shanghai, China) for chromatographic separation and then analyzed by Q-Exactive HF-X mass spectrometer (Thermo Scientific, Shanghai, China) to DDA mass spectrometry (Liu et al., 2021). Finally, the data were matched with the database by Proteome Discoverer software.

2.8 Statistical analysis

All data were analyzed three times and presented as means ± standard deviation. The statistical analysis was carried out using GraphPad Prism 8 software. A one-way repeated-measures analysis of variance with Duncan's multiple range test was applied to determine significant differences between means. The threshold *p*-value for significance was set at 0.05. The different letters (a, b, c, …) were used to express the significance when $p < 0.05$, and the same letter displayed there was no significance between groups ($p > 0.05$).

3 Results

3.1 Determination of the optimal conditions of three processing technologies of α-TM

The optimal conditions were explored (Supporting Information Fig. S1 ~ S3). The conditions of TG-catalyzed cross-linking, TG-catalyzed glycosylation, and glycation we selected in this study were: α-TM reacted with 1000 U/g TG at 37 °C, pH 8.5 for 3 h. The product was named α-TMT (Supporting Information Fig. S1A ~ S1F). α-TM and 50 U/g TG reacted with 1 mM GlcN at 37 °C, pH 6.5 for 1 h. The product was named α-TMGT (Supporting Information Fig. S2A ~ S2H). α-TM reacted with 0.6 mM Xyl at 100 °C, pH 8.5 for 0.5 h. The glycation with α-TM was named α-TMX (Supporting Information Fig. S3A ~ S3F).

Based on the confirmed conditions of the three processing technologies above, α-TM and its processed products were prepared for analysis by SDS-PAGE and Western blot (Fig. 1A and 1B). α-TMT and α-TMGT produced macromolecular substances > 180 kDa, whereas the MW of α-TMX increased slightly (Fig. 1A). The IgG-binding capacity of α-TMT, α-TMGT, and α-TMX decreased (Fig. 1B). As shown in Fig. 1C, the average particle size of α-TM was increased after three processing technologies, which was corresponding with SDS-PAGE. Due to different MW of α-TM after being processed, the average particle sizes of α-TM, α-TMT, α-TMGT, and α-TMX performed significant differences ($p < 0.05$), which were 265.5±9.9 nm, 927.4±3.54 nm, 775.3±14.0 nm, and 321.5±14.4 nm, respectively. The zeta potential of α-TM, α-TMT, α-TMGT, and α-TMX ranged from -10 mV to -25 mV (Fig. 1D). There was significant difference ($p < 0.05$) among the zeta potential of α-TM, α-TMT, α-TMGT, and α-TMX. However, it was no significance ($p > 0.05$) between α-TM and α-TMX, which indicated that α-TMX was as stable as α-TM in solution.

3.2 Secondary structure, surface hydrophobicity, and chemical bond analysis of α-TM and its processed products

The secondary structure of α-TM was mainly comprised of α-helix (Fig. 2A). Three

processing technologies had a noteworthy effect on the secondary structure of α-TM. The content of α-helix of α-TM was decreased significantly ($p < 0.05$) to 60.1±1.1%, 53.5±2.9%, and 42.0±2% respectively. The content of β-sheet was increased significantly ($p < 0.05$) to 5.6±0.8%, 6.4±1.5%, and 11.9±2.1% respectively. The content of β-turn was increased significantly ($p < 0.05$) to 14.4±0.7%, 15.5±0.7%, and 17.2±0.7% respectively. The content of the random coil was increased significantly ($p < 0.05$) to 19.8±0.2%, 24.5±3.5%, and 28.8±1.6% respectively (Fig. 2B). Moreover, the fluorescence intensity of the surface hydrophobicity of α-TMT, α-TMGT, and α-TMX was higher than α-TM. The fluorescence intensity peak of α-TM was blue-shifted after three processing technologies (Fig. 2C).

Fig. 2D showed that the principal chemical bond of α-TM was hydrophobic force. Three processing technologies significantly reduced the content of hydrophobic force. α-TMT performed the lowest hydrophobic force. The hydrogen bond content of α-TMT was increased significantly ($p < 0.05$). The contents of the disulfide bond of α-TMT, α-TMGT, and α-TMX were increased significantly ($p < 0.05$). The disulfide bond content of α-TMGT was the highest. The spatial structure of α-TMX was maintained by hydrophobic force and hydrogen bond, as a whole.

3.3 Analysis of the reacted degree and glycan bond type of α-TM after three processing technologies

The wavelength scanning of α-TM and its processed products was measured using UV absorption spectra (Fig. 2E). It was found that the highest absorption peak of α-TMT, α-TMGT, and α-TMX performed a slight blue shift, and a new absorption peak appeared at about 273 nm. The new absorption peak values were 9.13±0.05, 4.30±0.03, and 7.91±0.01, respectively. To analyze the characteristic absorption peak of the glycated α-TM at the primary, middle, and final periods, the optical density at 294 nm,

320 nm, and 420 nm were visualized in Supporting Information Table S1. Compared with α-TM, α-TMX was owned mainly by the primary products of glycation. Meanwhile, after the NaOH treatment, the optical density of α-TMT and α-TMGT were higher, which indicated that both α-TMT and α-TMGT were linked by the O-glycan bonds (Fig. 2F and 2G). Oppositely,-the N-glycan bonds linked between α-TM and Xyl during glycation (Fig. 2H).

3.4 Immunoreactivity analysis of α-TM and its processed products

Three processing technologies reduced significantly the IgG/IgE-binding capacity (Fig. 3A). The IgG-binding capacity of α-TMT, α-TMGT, and α-TMX decreased by 25.9±0.5%, 25.6±4.7% and 37.9±0.4% respectively, and the IgE-binding capacity also decreased by 43.5±9.3%, 18.8±1.0% and 70.1±10.4% respectively, when compared with α-TM. Glycation can reduce the IgG/IgE-binding capacity of α-TM effectively ($p < 0.05$).

The inhibition rates of α-TM, α-TMT, α-TMGT, and α-TMX were shown in Fig. 3B. It was found that the IC_{50} of α-TM, α-TMT, α-TMGT, and α-TMX were 0.16 μg/mL, 1.30 μg/mL, 10.55 μg/mL, and 40.24 μg/mL, respectively. The IC_{50} value of α- TM/α-TMX was 251.5 times, which indicated α-TMX performed the lowest immunoreactivity.

3.5 Analysis of the ability of site-specific IgE to recognize epitope peptides

α-TMT, α-TMGT, and α-TMX could only bind with part of IgE when α-TM could bind with IgE most. The site-specific IgE showed a lower ability to bind with α-TM in comparison to the IgE that was without any treatment (Fig. 4A). It was found that the binding capacity of seven IgE linear epitope peptides to specific sera was different through inhibition dot blot analysis (Fig. 4B). It would be proved that this epitope peptide could bind with IgE whereas the processed products could not when the

intensity of the dots on the membrane was weak. L-HTM-1 could bind with IgE, which proved that part of L-HTM-1 of α-TMT was modified or destroyed. The intensity of the dots on the membrane was weak when the peptides (L-HTM-1 and L-HTM-2) were added to the site-specific IgE prepared by α-TMT. Glycation reduced the binding capacity of L-HTM-2, L-HTM-3, L-HTM-4, L-HTM-6, and L-HTM-7 with site-specific IgE.

3.6 Analysis of the amino acid frequency of linear epitopes and the whole protein

Fig. 4C showed that the content of Glutamate was the highest, followed by Alanine, Leucine, and Lysine, with the analysis of the α-TM and verified epitopes (Supporting Information Table S2). Meanwhile, Glutamine, Lysine, Asparagine, and Arginine were relative-high distributed in epitope by heatmap analysis (Fig. 4D). These amino acids might be modified after processing technologies.

3.7 Modification of α-TM specific amino acids after glycation

The modification of specific amino acids of α-TM was analyzed using EASY nLC 1200 and Q Exactive (Fig. 5A). The methods to modify the amino acids by glycation were as follows: Deamidated:18O, Oxidation, and Carbamidomethyl. The glycated sites were shown in Supporting Information Table S3. Nine amino acids (M13, N17, N44, C50, N55, M68, N102, N202, and N203) were fully modified and five amino acids (M8, N11, N25, C45, and N52) were not fully modified. The modified amino acids were mapped to the three-dimensional (3D) structure of α-TM (Fig. 5B) to find that L-HTM-1, L-HTM-3, and L-HTM-7 were modified-and the sites on epitopes were N11, M13, N17, N25, M68, N202, and N203.

4 Discussion

Allergy to shellfish is common throughout life continuously and has a significant effect on daily life (Sicherer, Warren, Dant, Gupta, & Nadeau, 2020). Abalone allergy

has been a growing concern in recent years, and it is hard to avoid (Suzuki, Kobayashi, Hiraki, Nakata, & Shiomi, 2011; Suh, Kim, Kim, Kim, & Kim, 2020). As a pan-allergen in abalone, the allergic reaction to TM cannot be overlooked. The research of processing technologies with hypo-immunoreactivity for TM from abalone is urgent and instant.

The enzymic cross-linking reaction, enzyme-catalyzed glycosylation, and glycation are promising approaches that can reduce the allergenicity of proteins from shellfish (Ahmed et al., 2021; Yuan, Lv, Li, Mi, Chen, & Lin, 2016; Bai et al., 2021). However, the type of reagent concentration, intrinsic characteristics of the allergen, reacted temperature, time, and pH can decrease or increase the immunoreactivity to some extent (He et al., 2020; Gupta, Gupta, Sharma, Das, Ansari, & Dwivedi, 2018). Met e 1 was incubated in 50 mM PBS (pH 7.4) at 37 °C for 12 h with 200 U/g TG, which resulted in a reduction of 49.1% (IgG) and 63.4% (IgE) (Ahmed et al., 2020). Fu et al. (2019) reduced the immunoreactivity of TM from *Penaeus chinensis* by optimizing the TG-catalyzed cross-linking reaction of to confirm the conditions as follows: 1000 U/mg TG with TM reacted at 37 °C for 16-24 h. Besides, Yuan et al. (2016; 2018) reported that TG and GlcN are suitable for enzyme-catalyzed glycosylation to decrease the immunoreactivity of protein. However, TG-catalyzed cross-linking reaction and TG-catalyzed glycosylation had little effect on reducing the immunoreactivity of α-TM. It was due to the short time during processing. TG-catalyzed cross-linking reaction and TG-catalyzed glycosylation with α-TM was 3 h and 1 h, respectively. The reaction time was selected to make the processed products safer, which was shorter than those of TM from shrimp. Thus, it could be speculated that the more reaction time to be analyzed in this study could perform the lower immunoreactivity, such as the processed TM from shrimp. It was found that Arab, Glu, and Gal could also reduce the IgE reactivity of TM

306 from shellfish with different processed conditions (Nakamura, Watanabe, Ojima, Ahn,
307 & Saeki, 2005; Fu, Wang, Wang, Ni, & Wang, 2019; Han et al., 2018). In this study,
308 immunoreactivity was reduced significantly ($p < 0.05$) for α-TM reacting with 0.6 mM
309 Xyl (pH 8.5) at 100 °C for 0.5 h, which was consistent with the result of TM from the
310 scallop (Bai et al., 2021). Both scallop and abalone belong to mollusks, TM from same
311 source might showed the similar processing result. It indicated that glycation with Xyl
312 might be suitable for decreasing the immunoreactivity of TM from oyster, clam, and
313 other mollusks.

314 The content of α-helix in α-TM was decreased significantly ($p < 0.05$) during
315 processing, especially in α-TMX. It was studied that the changes in the α-helix structure
316 could mediate the reduction of allergenicity (Gou, Liang, Huang, & Ma, 2022). Ara h
317 1 was cross-linked by TG, which was stabilized mainly by hydrogen bonds, and the
318 content of hydrophobic force was decreased (Tian, Liu, Xue, & Wang, 2020); this result
319 is consistent with α-TMT. TG-catalyzed cross-linking reaction would affect the
320 immunoreactivity of protein by changing the proportion of chemical bonds.
321 Interestingly, when the content of hydrophobic force decreased significantly ($p < 0.05$),
322 the hydrophobicity intensity increased; the two parameters were negatively correlated.
323 That may be due to the exposure of the intermolecular-hydrophobic groups during
324 processing. The absorption peak of α-TM performed a slight blue shift after three
325 processing technologies, which indicated that structural modifications or
326 conformational changes could have occurred (Liu et al., 2020). The displacement of
327 absorption has related to the exposure of chromophoric groups. The chromophoric
328 amino acids (Tyrosine, and Phenylalanine) were found in the sequence of α-TM. The
329 zeta potential of α-TMX was not significant with α-TM ($p > 0.05$), although α-TMX
330 performed the most obvious alternation in structure. Mahdavian, & Arash (2021) found

that the surface hydrophobicity of GPPINPs increased while their solubility decreased. The decreased solubility meant that the samples were not stable in solution and the absolute value of zeta potential were low. The surface hydrophobicity intensity of α-TMX showed the minimum increase. That may be the reason for the no significance between α-TM and α-TMX, while there was significant among α-TM, α-TMT, and α-TMGT.

The spatial structure is closely related to the allergenicity of proteins (Wai et al., 2020). IgG/IgE-binding capacity is often used to assess the effect of the processing on allergens (Zhang, Xiao, Zhang, & Zhou, 2018; Zhang, Li, Xiao, Nowak-Wegrzyn, & Zhou, 2020). The IgG/IgE-binding capacity of α-TM was decreased, especially after glycation. It was found that the content of α-helix decreased when the IgG/IgE-binding capacity of α-TM was reduced, combined with the changes of structure. Although there is no positive correlation between α-helix content and IgG/IgE-binding capacity, the decrease of the α-helix structure may be one reason for the lowest IgG/IgE-binding capacity of glycated α-TM. It could be concluded that the structure alternation might influence the binding capacity between allergen and antibody. Thus, Xi et al. (2020) prepared the site-specific IgG to confirm the destroyed epitopes. The same method of preparation of site-specific IgE was used in this research. The IgG/IgE-binding capacity remained when the epitopes existed in the processed allergen to bind with IgE (Rahaman, Vasiljevic, & Ramchandran, 2016). Further analysis revealed that L-HTM-1 could bind with the site-specific IgE prepared by TG-catalyzed cross-linking to prove being mainly modified or destroyed during TG-catalyzed cross-linking. Similar results were found that L-HTM-1 and L-HTM-2 were mainly modified or destroyed during TG-catalyzed glycosylation, and five epitope peptides were modified or destroyed during glycation. Among them, L-HTM-4 and L-HTM-6 were the dominant linear

356 epitopes due to their great capacity to bind with IgE (Ji et al., 2021); this suggested that
357 the loss of the IgE-binding capacity of important epitopes could result in weaker IgE-
358 binding capacity. The reduction of the proportion of α-helix changed the capacity of
359 epitopes to bind with IgE, and then decreased the immunoreactivity of α-TM.

360 Both the N-glycan and O-glycan were found in TM from *Exopalaemon modestus*
361 (Zhang, Xiao, Zhang, & Zhou, 2019). Interestingly, α-TM had the N-glycan bond after
362 glycation, whereas the O-glycan bond was found in α-TM after TG-catalyzed cross-
363 linking and TG-catalyzed glycosylation. The site of the N-glycan bond is Asparagine.
364 Nine modified sites (M13, N17, N44, C50, N55, M68, N102, N202, and N203) were
365 identified. The results indicated that the modified sites of glycation are not only Lysine
366 and Arginine. Not only that, three glycated sites were mapped on the L-HTM-3 and L-
367 HTM-7, and two epitope peptides suffered the binding capacity of the site-specific IgE.
368 Although M13 and M17 were located on L-HTM-1, there was no influence on the
369 binding capacity of the peptides with the site-specific IgE. That may be because M13
370 and M17 were not key amino acids on L-HTM-1.

371 Besides, many researchers found that sugar conjugation could reducing the
372 allergenicity of proteins by modifying the epitopes (Han et al., 2022; Bai et al., 2021).
373 Although TM from shellfish has a low homology (over 60%), Lysine and Arginine
374 displayed the same positions in the whole sequence. The number of the same sites
375 (Lysine and Arginine) was about 70% (Han et al., 2018; Han et al., 2022) in comparison
376 to the modified sites of TM from the crab after glycation with Arab or Gal. It could
377 deduce that the glycated α-TM might perform the same modified sites. Meanwhile, the
378 modified sites on the IgE epitopes of TM from scallop (glycated with Xyl) were K12,
379 R15, K28, K76, R125, R127, K128, R133, R140, K146, and K189 (Bai et al., 2021),
380 which were also on the sequence of α-TM. Another three epitopes could bind with the

site-specific IgE that needs further confirmation. It was suggested the possible destruction or modification of the IgE epitopes would influence its capacity to bind with IgE by glycation. There was little research on identifying the modified sites after TG-catalyzed cross-linking reaction and TG-catalyzed glycosylation. Most of the reported modified amino acids by TG-catalyzed cross-linking were Glutamine and Arginine, and by TG-catalyzed glycosylation was only Glutamine (Tian, Liu, Xue, & Wang, 2020) which were located on epitopes. Hence, future research in our laboratory will also concentrate on verifying the modified sites of α-TM after glycation, TG-catalyzed cross-linking, and TG-catalyzed glycosylation using mass spectrometry. Meanwhile, the hypo-allergenicity analysis and the oral tolerance of the processed products *in vivo* using a mouse model is worthy of exploration.

5 Conclusion

In conclusion, not only the contents of α-helix were decreased, but also the surface hydrophobicity of α-TM was increased by TG-catalyzed cross-linking, TG-catalyzed glycosylation, and glycation. The glycated α-TM with Xyl performed the lowest IgG/IgE-binding capacity. Five of seven epitope peptides could bind with the site-specific IgE that was prepared by the glycated α-TM. Finally, nine specific amino acids on glycated α-TM were verified. Three modified sites were located on two epitopes (L-HTM-3 and L-HTM-7) to affect the IgE-binding capacity of α-TM to a certain extent. The results provide new research methods for exploring hypoallergenic abalone, which will be used for oral tolerance.

CRediT authorship contribution statement

Nairu Ji: Conceptualization, Methodology, Validation, Investigation, Formal analysis, Writing - original draft, Visualization. **Chenchen Yu:** Investigation, Data curation. **Xinyu Han:** Conceptualization, Methodology. **Xinrong He:** Methodology. **Shuai Kang:** Methodology. **Tianliang Bai:** Investigation. **Hong Liu:** Investigation. **Guixia Chen:** Resources. **Minjie Cao:** Supervision, Writing - review & editing. **Guangming Liu:** Writing - review & editing, Supervision, Project administration, Funding acquisition.

Declaration of competing interest

The authors declare that they have no known competing financial interests or personal relationships that could have appeared to influence the work reported in this paper.

Acknowledgements

This work was supported by the National Natural Scientific Foundation of China (grant numbers 32072336, 31871720), and the National Key R&D Program of China (grant number 2019YFD0901703). The technical support was provided by Shanghai Bioprofile Technology Company Ltd.

Appendix A. Supplementary data

For additional experimental results, see Supplementary data. Optimization of TG-catalyzed cross-linking reacted α-TM (Figure S1), optimization of TG-catalyzed glycosylated α-TM (Figure S2), optimization of glycated α-TM (Figure S3), characteristics absorption of α-TM and its processed products (Table S1), information

423 about the identified linear epitopes of α-TM (Table S2), and Identification of glycation

424 modified sites of α-TM (Table S3).

References

Ahmed, I., Lin, H., Xu, L. L., Li, S., Costa, J., Mafra, I., … Li, Z. X. (2020). Immunomodulatory effect of laccase/caffeic acid and transglutaminase in alleviating shrimp tropomyosin (Met e 1) allergenicity. *Journal of Agricultural and Food Chemistry*, *68*(29), 7765-7778. https://doi.org/10.1016/10.1021/acs.jafc.0c02366.

Ahmed, I., Lin, H., Li, Z. X., Xu, L. L., Qazi, I. M., Luo, C., … Sun, L. R. (2021). Tyrosinase/caffeic acid cross-linking alleviated shrimp (*Metapenaeus ensis*) tropomyosin-induced allergic responses by modulating the Th1/Th2 immunobalance. *Food Chemistry*, *340*, 127948. https://doi.org/10.1016/j.foodchem.2020.127948.

Anvari, S., Miller, J., Yeh, C. Y., & Davis, C. M. (2019). IgE-mediated food allergy. *Clinical Reviews in Allergy & Immunology*, *57*(2), 244-260. https://doi.org/10.1007/s12016-018-8710-3.

Bai, T. L., Han, X. Y., Li, M. S., Yang, Y., Liu, M., Ji, N. R., … Liu, G. M. (2021). Effects of the Maillard reaction on the epitopes and immunoreactivity of tropomyosin, a major allergen in *Chlamys nobilis*. *Food & Function*, *12*(11), 5096-5108. https://doi.org/10.1039/d1fo00270h.

Costa, J., Bavaro, S. L., Benede, S., Diaz-Perales, A., Bueno-Diaz, C., Gelencser, E., …, Holzhauser, T. (2022). Are physicochemical properties shaping the allergenic potency of plant allergens? *Clinical Reviews in Allergy & Immunology*, *62*(1), 37-63. https://doi.org/10.1007/s12016-020-08826-1.

Faber. M. A., Pascal, M., El Kharbouchi, O., Sabato, V., Hagendorens, M. M., Decuyper, I. I., … Ebo, D. G. (2017). Shellfish allergens: Tropomyosin and beyond. *Allergy*, *72*(6), 842-848.

https://doi.org/10.1111/all.13115.

Faisal, M., Vasiljevic, T., & Donkor, O. N. (2019). Effects of selected processing treatments on antigenicity of banana prawn (*Fenneropenaeus merguiensis*) tropomyosin. *International Journal of Food Science and Technology*, *54*(1), 183-193. https://doi.org/10.1111/ijfs.13922.

Fu, L. L., Ni, S. Q., Wang, C., & Wang, Y. B. (2019). Transglutaminase-catalysed cross-linking eliminates *Penaeus chinensis* tropomyosin allergenicity by altering protein structure. *Food and Agricultural Immunology*, *30*(1), 296-308. https://doi.org/10.1080/09540105.2019.1580250.

Fu, L. L., Wang, C., Wang, J., Ni, S. Q., & Wang, Y. B. (2019). Maillard reaction with ribose, galacto-oligosaccharide or chitosan-oligosaccharide reduced the allergenicity of shrimp tropomyosin by inducing conformational changes. *Food Chemistry*, *274*, 789-795. https://doi.org/10.1016/j.foodchem.2018.09.068.

Gou, J. K., Liang, R., Huang, H. J., & Ma, X. J. (2022). Maillard reaction induced changes in allergenicity of food. *Foods*, *11*(4), 530. https://doi.org/10.3390/foods11040530.

Gupta, R. K., Gupta, K., Sharma, A., Das, M., Ansari, I. A., & Dwivedi, P. D. (2018). Maillard reaction in food allergy: Pros and cons. C*ritical Reviews in Food Science and Nutrition*, *58*(2), 208-226. https://doi.org/10.1080/10408398.2016.1152949.

Han, X. Y., Yang, H., Rao, S. T., Liu, G. Y., Hu, M. J., Zeng, B. C., … Liu, G. M. (2018). The Maillard reaction reduced the sensitization of tropomyosin and arginine kinase from *Scylla paramamosain*, simultaneously. *Journal of Agricultural and Food Chemistry*, *66*(11), 2934-2943. https://doi.org/10.1021/acs.jafc.7b05195.

Han, X. Y., Bai, T. L., Yang, H., Lin, Y. C., Ji, N. R., Wang, Y. B., … Liu, G. M. (2022). Reduction in allergenicity and induction of oral tolerance of glycated tropomyosin from crab. *Molecules*, *27*(6), 2027. https://doi.org/ 10.3390/molecules27062027.

He, W. Y., He, K., Sun, F., Mu, L. X., Liao, S. T., Li, Q. R., … Wu, X. L. (2020). Effect of heat, enzymatic hydrolysis and acid-alkali treatment on the allergenicity of silkworm pupa protein extract. *Food Chemistry*, *343*, 128461. https://doi.org/10.1016/j.foodchem.2020.128461.

Ho, M. H. K., Wong, W. H. S., & Chang, C. (2014). Clinical spectrum of food allergies: A comprehensive review. *Clinical Reviews in Allergy & Immunology*, *46*(3), 225-240. https://doi.org/10.1007/s12016-012-8339-6.

Hrynets, Y., Ndagijimana, M., & Betti, M. (2013). Transglutaminase-catalyzed glycosylation of natural actomyosin (NAM) using glucosamine as amine donor: Functionality and gel microstructure. *Food Hydrocolloids*, 36, 26-36. https://doi.org/10.1016/j.foodhyd.2013.09.001.

Ji, N. R., Han, X. Y., Yu, C. C., Wang, Y. J., He, X. R., Liu, H., … Liu, G. M. (2021). Analysis of immunoreactivity of α/α_2-tropomyosin from *Haliotis discus hannai*, based on IgE epitopes and structural characteristics. *Journal of Agricultural and Food Chemistry*, *69*(50), 15403-15413. https://doi.org/10.1021/acs.jafc.1c06401.

Jin, Y. F., Deng, Y., Qian, B. J., Zhang, Y. F., Liu, Z. M., & Zhao, Y. Y. (2015). Allergenic response to squid (*Todarodes pacificus*) tropomyosin Tod p1 structure modifications induced by high hydrostatic pressure. *Food and Chemical Toxicology*, *76*, 86-93. https://doi.org/10.1016/j.fct.2014.12.002.

Liu, C., & Sathe, S. K. (2018). Food allergen epitope mapping. *Journal of Agricultural and Food Chemistry*, *66*(28), 7238-7248. https://doi.org/10.1021/acs.jafc.8b01967.

Liu, M., Liu, S. H., Han, T. J., Xia, F., Li, M. S., Weng, W. Y., … Liu, G. M. (2019). Effects of thermal processing on digestion stability and immunoreactivity of the *Litopenaeus vannamei* Matrix. *Food & Function, 10*(9), 5374-5385. https://doi.org/10.1039/c9fo00971j.

Liu, M., Huan, F., Li, M. S., Han, T. J., Xia, F., Yang, Y., … Liu, G. M. (2021). Mapping and IgE-binding capacity analysis of heat/digested stable epitopes of mud crab allergens. *Food Chemistry*, *344*, 128735-128743. https://doi.org/10.1016/j.foodchem.2020.128735.

Mahdavian, M. H., & Arash, K. (2021). Physicochemical properties of Grass pea (*Lathyrus sativus L.*) protein nanoparticles fabricated by cold atmospheric-pressure plasma. *Food Hydrocolloids*, *112*, 106328. https://doi.org/10.1016/j.foodhyd.2020.106328.

Nakamura, A., Watanabe, K., Ojima, T., Ahn, D.H., & Saeki, H. (2005). Effect of Maillard reaction on allergenicity of scallop tropomyosin. *Journal of Agricultural and Food Chemistry*, *53*(19), 7559-7564. https://doi.org/ 10.1021/jf0502045.

Poms, A., Davies, J. M., Gadermaier, G., Hilger, C., Holzhauser, T., Lidholm, J., … Goodman, R. E. (2018). WHO/IUIS allergen nomenclature: Providing a common language. *Molecular Immunology*, *100*, 3-13. https://doi.org/10.1016/j.molimm.2018.03.003.

Rahaman, T., Vasiljevic, T., & Ramchandran, L. (2016). Effect of processing on conformational changes of food proteins related to allergenicity. *Trends In Food Science & Technology*, *49*, 24-34. https://doi.org/10.1016/j.tifs.2016.01.001.

Ruan, W. W., Cao, M. J., Chen, F., Cai, Q. F., Su, W. J., Wang, Y. Z., … Liu, G. M. (2013). Tropomyosin contains IgE-binding epitopes sensitive to periodate but not to enzymatic

513 deglycosylation. *Journal of Food Science*, *78*(8), C1116-C1121.
514 https://doi.org/10.1111/1750-3841.12169.

515 Shen, H. W., Cao, M. J., Cai, Q. F., Ruan, M. M., Mao, H. Y., Su, W. J., … Liu, G. M. (2012).
516 Purification, cloning, and immunological characterization of arginine kinase, a novel
517 allergen of *Octopus fangsiao*. *Journal of Agricultural and Food Chemistry*, *60*(9), 2190-
518 2199. https://doi.org/10.1021/jf203779w.

519 Sicherer, S. H., Warren, C. M., Dant, C., Gupta, R. S., & Nadeau, K. C. (2020). Food allergy from
520 infancy through adulthood. *The Journal of Allergy and Clinical Immunology in Practice*,
521 *8*(6), 1854-1864. https://doi.org/10.1016/j.jaip.2020.02.010.

522 Suh, S. M., Kim, M. J., Kim, H. I., Kim, H. J., &Kim, H. Y. (2020). A multiplex PCR assay
523 combined with capillary electrophoresis for the simultaneous detection of tropomyosin
524 allergens from oyster, mussel, abalone, and clam mollusk species. *Food Chemistry*, *317*,
525 126451. https://doi.org/10.1016/j.foodchem.2020.126451.

526 Suzuki, M., Kobayashi, Y., Hiraki, Y., Nakata, H., & Shiomi, K. (2011). Paramyosin of the disc
527 abalone *Haliotis discus discus*: Identification as a new allergen and cross-reactivity with
528 tropomyosin. *Food Chemistry*, *124*(3), 921-926.
529 https://doi.org/10.1016/j.foodchem.2010.07.020.

530 Thaiphanit S, Schleining G, Anprung P. (2016). Effects of coconut (*Cocos Nucifera L.*) protein
531 hydrolysates obtained from enzymatic hydrolysis on the stability and rheological properties
532 of oil-in-water emulsions. *Food Hydrocolloids*, *60*, 252-264.
533 https://doi.org/10.1016/j.foodhyd.2016.03.035.

534 Tian, Y., Liu, C. L., Xue, W. T., & Wang, Z. F. (2020). Crosslinked recombinant-Ara h 1 catalyzed
535 by microbial transglutaminase: Preparation, structural characterization and allergic

assessment. *Foods*, *9*(10), 1508. https://doi.org/10.3390/foods9101508.

Wai, C. Y. Y., Leung, N. Y. H., Chu, K. H., Leung, P. S. C., Leung, A. S. Y., Wong, G. W. K., … Leung, T. F. (2020). Overcoming shellfish allergy: How far have we come? *International Journal of Molecular Sciences*, *21*(6), 2234. https://doi.org/10.3390/ijms21062234.

Xi, J., & He, M. X. (2020). Location of destroyed antigenic sites of Gly m Bd 60 K after three processing technologies. *Food Research International*, *134*, 109-119. https://doi.org/10.1016/j.foodres.2020.109199.

Yang, Y., Hu, M. J., Jin, T. C., Zhang, Y. X., Liu, G. Y., Li, Y. B., … Liu, G. M. (2019). A comprehensive analysis of the allergenicity and IgE epitopes of myosinogen allergens in *Scylla paramamosain*. *Clinical and Experimental Allergy*, *49*(1), 108-119. https://doi.org/10.1111/cea.13266.

Yuan, F. Z., Lv, L. T., Li, Z. X., Mi, N. S., Chen, H. R., & Lin, H. (2016). Effect of transglutaminase-catalyzed glycosylation on the allergenicity and conformational structure of shrimp (*Metapenaeus ensis*) tropomyosin. *Food Chemistry*, *219*, 215-222. https://doi.org/10.1016/j.foodchem.2016.09.139.

Yuan, F. Z., Ahmed, I., Lv, L. T., Li, Z. X., Li, Z. X., Lin, H., … Ma, J. J. (2018). Impacts of glycation and transglutaminase-catalyzed glycosylation with glucosamine on the conformational structure and allergenicity of bovine beta-lactoglobulin. *Food & Function*, *9*(7), 3944-3955. https://doi.org/10.1016/10.1039/c8fo00909k.

Zhang, Z. Y., Xiao, H., Zhang, X. F., & Zhou, P. (2019). Conformation, allergenicity and human cell allergy sensitization of tropomyosin from *Exopalaemon modestus*: Effects of deglycosylation and Maillard reaction. *Food Chemistry*, *276*, 520-527.

https://doi.org/10.1016/j.foodchem.2018.10.032.

Zhang, Z. Y., Li, X. M., Xiao, H., Nowak-Wegrzyn, A., & Zhou, P. (2020). Insight into the allergenicity of shrimp tropomyosin glycated by functional oligosaccharides containing advanced glycation end products. *Food Chemistry*, *302*, 125348. https://doi.org/10.1016/10.1016/j.foodchem.2019.125348.

563 Table 1. Age, sex, specific IgE levels, and symptoms of the abalone-sensitized patients.

No.	Age (years)	Sex	Specific IgE of f_{22} (kU/L) [a]	Specific IgE of α-TM (OD 450 nm) [b]	Symptoms
1	33	F	25.53	0.19	Acute bronchitis
2	17	M	14.17	0.15	Eczema
3	9	F	19.66	0.15	Cough
4	32	M	5.61	0.16	Nausea and vomiting
5	29	M	12.72	0.14	Atopic dermatitis
6	27	F	9.81	0.17	Eczema
7	29	M	7.17	0.13	Urticaria
8	24	F	31.36	0.15	Lungs infected
9	18	F	3.91	0.17	Anaphylactic rhinitis
10	31	M	9.19	0.18	Cough
11[c]	22	F	0.11	0.06	-[d]
12[c]	18	M	0.19	0.07	-[d]

564 [a] A sera with specific IgE of $f_{22} \geq 0.35$ kU/L is defined as potential-positive. [b] A sera with OD 450

565 nm of α-TM ≥ 0.10 is defined as abalone-sensitized sera, when the OD 450 nm of sera from

566 nonallergic individual is 0.06 or 0.07. [c] A person was nonallergic individual. [d] A nonallergic

567 individual was nonallergic symptom. M, male; F, female.

Figure legends

Figure 1. Effects of three processing technologies on MW, average particle size, and zeta potential of α-TM.

A-B: SDS-PAGE (A) and Western blot (B) assays of α-TM treated by TG-catalyzed crosslinking reaction, TG-catalyzed glycosylation, and glycation, respectively.

Lane M: protein marker; lane 1: α-TM without treatment; lane 2: α-TM treated by enzymatic crosslinking reaction; lane 3: α-TM treated by TG-catalyzed glycosylation; lane 4: α-TM treated by glycation.

C-D: Average particle size (C) and zeta potential (D) analysis of α-TM treated by TG-catalyzed crosslinking reaction, TG-catalyzed glycosylation, and glycation, respectively.

All data are presented as the means ± standard deviation. The significance ($p < 0.05$) is precised as different letters (a, b, c, and d). The average particle size and zeta potential of α-TM, α-TMT, α-TMGT, and α-TMX were showed by white, green, blue, and black, respectively.

Figure 2. Effects on the structure of α-TM after three processing technologies.

A-B: Secondary structure (A) and its contents (B) analysis of α-TM, α-TMT, α-TMGT, and α-TMX.

All data are presented as the means ± standard deviation. The significance ($p < 0.05$) among the content of each secondary structure of α-TM, α-TMT, α-TMGT, and α-TMX is precised as different letters (a, b, c, …). The content of each secondary structure of α-TM, α-TMT, α-TMGT, and α-TMX were showed by white, green, blue, and black, respectively.

C-E: The surface hydrophobicity(C), chemical bond (D), and wavelength scanning(E) analysis of α-TM, α-TMT, α-TMGT, and α-TMX.

All data are presented as the means ± standard deviation. The significance ($p < 0.05$) among the content of each s chemical bond of α-TM, α-TMT, α-TMGT, and α-TMX is precised as different letters (a, b, c, …). The content of the chemical bond of α-TM, α-TMT, α-TMGT, and α-TMX were showed by white, green, blue, and black, respectively.

F-H: Determination of the major type of the glycan bond of α-TMT (F), α-TMGT (G), and α-TMX (H).

α-TMT treated, α-TMGT treated, and α-TMX treated presented α-TMT, α-TMGT, and α-TMX treated with NaOH to measure the type of glycan bond, respectively.

Figure 3. IgG/IgE-binding capacity analysis of α-TM after three processing technologies.

A: IgG/IgE-binding capacity analysis of α-TM, α-TMT, α-TMGT, and α-TMX.

The rabbit anti-*H. discus hannai* TM polyclonal antibody and abalone-sensitized patients' serum pool were used in ELISA. The serum pool includes serum No.1 ~ 10 from Table 1. All data are presented as the means ± standard deviation. The significance ($p < 0.05$) is precised as different letters (a, b, and c). The IgG/IgE-binding capacity of α-TM, α-TMT, α-TMGT, and α-TMX were showed by white, green, blue, and black, respectively.

B: IgG-binding capacity analysis of α-TM, α-TMT, α-TMGT, and α-TMX.

The rabbit anti-*H. discus hannai* TM polyclonal antibody was used in inhibition ELISA. α-TM on the solid phase; α-TM, α-TMT, α-TMGT, and α-TMX as the inhibitor respectively.

Figure 4. Effects of linear epitopes on α-TM after three processing technologies.

A: Preparation of the site-specific IgE.

The NC group was that BSA was doted on the nitrocellulose membrane as the negative control, and number 1 ~ 2 using negative serum (No.11 ~ 12), the number 3 ~ 4 using positive serum pool (No.1 ~ 10). The PC group was that α-TM, α-TMT, α-TMGT, and α-TMX (number 1 ~ 4) was doted on the nitrocellulose membrane as the positive control, and the primary antibody was positive serum pool (No.1 ~ 10). The Con group was that α-TM was doted on the nitrocellulose membrane, and the site-specific IgE that was prepared by adding α-TM, α-TMT, α-TMGT, and α-TMX as the inhibitor (the number 1 ~ 4). All the serum were diluted with 1:3.

B: Determination of the epitope peptides that could bind with the prepared site-specific IgE.

α-TM, α-TMT, α-TMGT, and α-TMX were represented the first inhibitor to prepare the site-specific IgE, and the number 1 ~ 7 represented L-HTM-1 ~ L-HTM-7 as the second inhibitor to be added in the site-specific IgE respectively; α-TM was doted on the nitrocellulose membrane.

C: Amino acid frequency of the whole protein and the linear epitopes of α-TM.

D: Heatmap analysis of the amino acid in the linear epitopes of α-TM.

Figure 5. Identification of modification sites of α-TM after glycation.

A: Identification of the modified specific amino acids of the glycated α-TM using N-

626 glycosylation Proteomics.

627 B: Map of the identified modification sites on the 3D structure of α-TM.

628 **Figure 1**

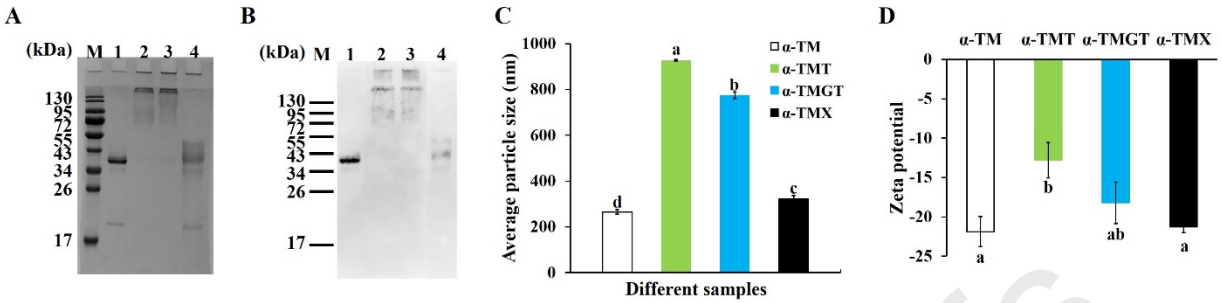

629

630 **Figure 2**

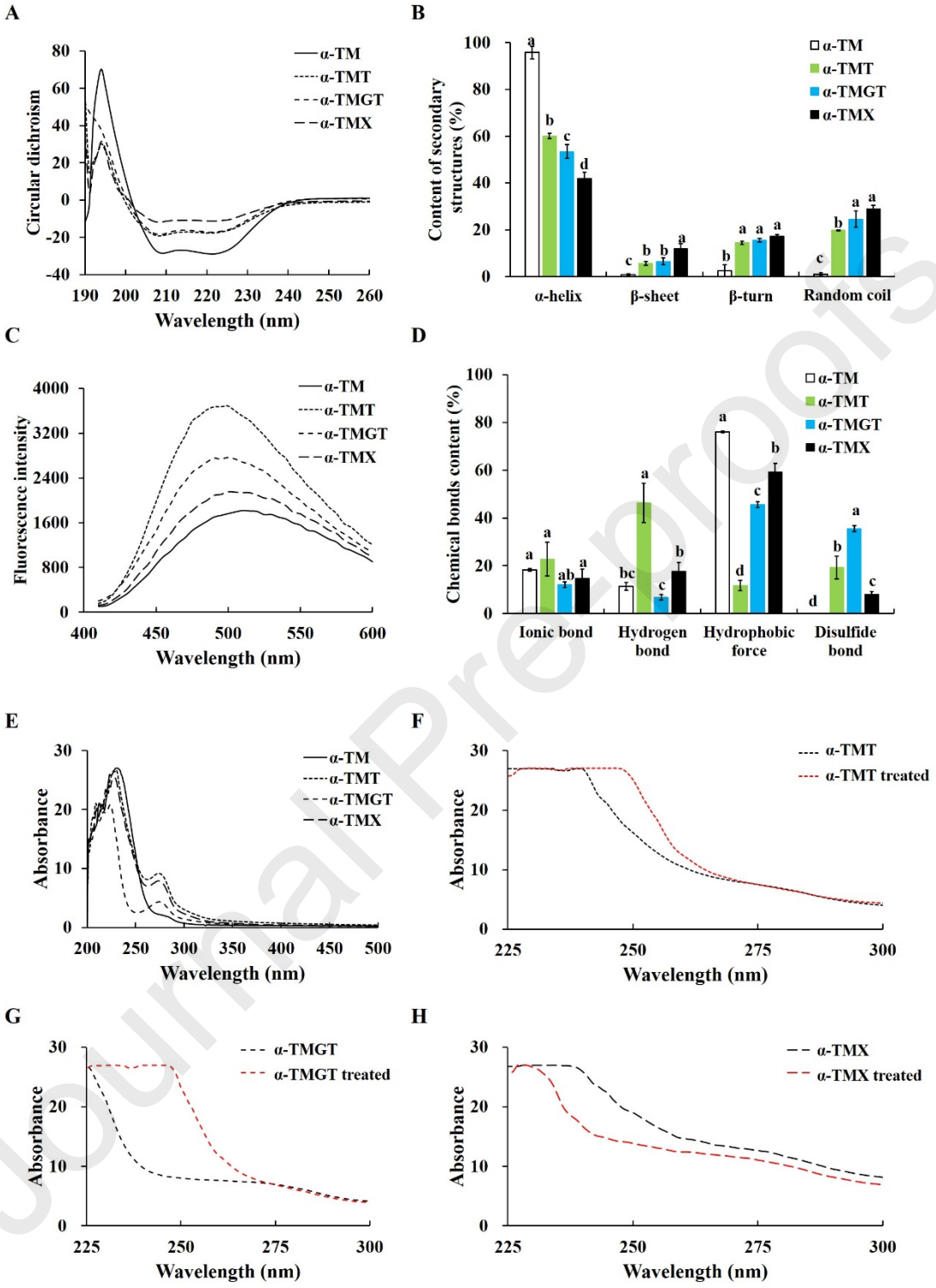

631

632 **Figure 3**

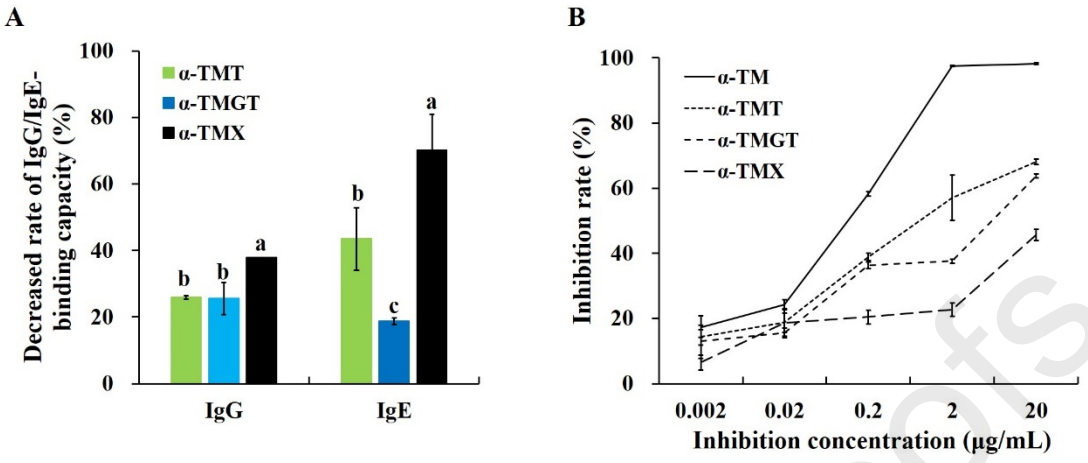

633

634 **Figure 4**

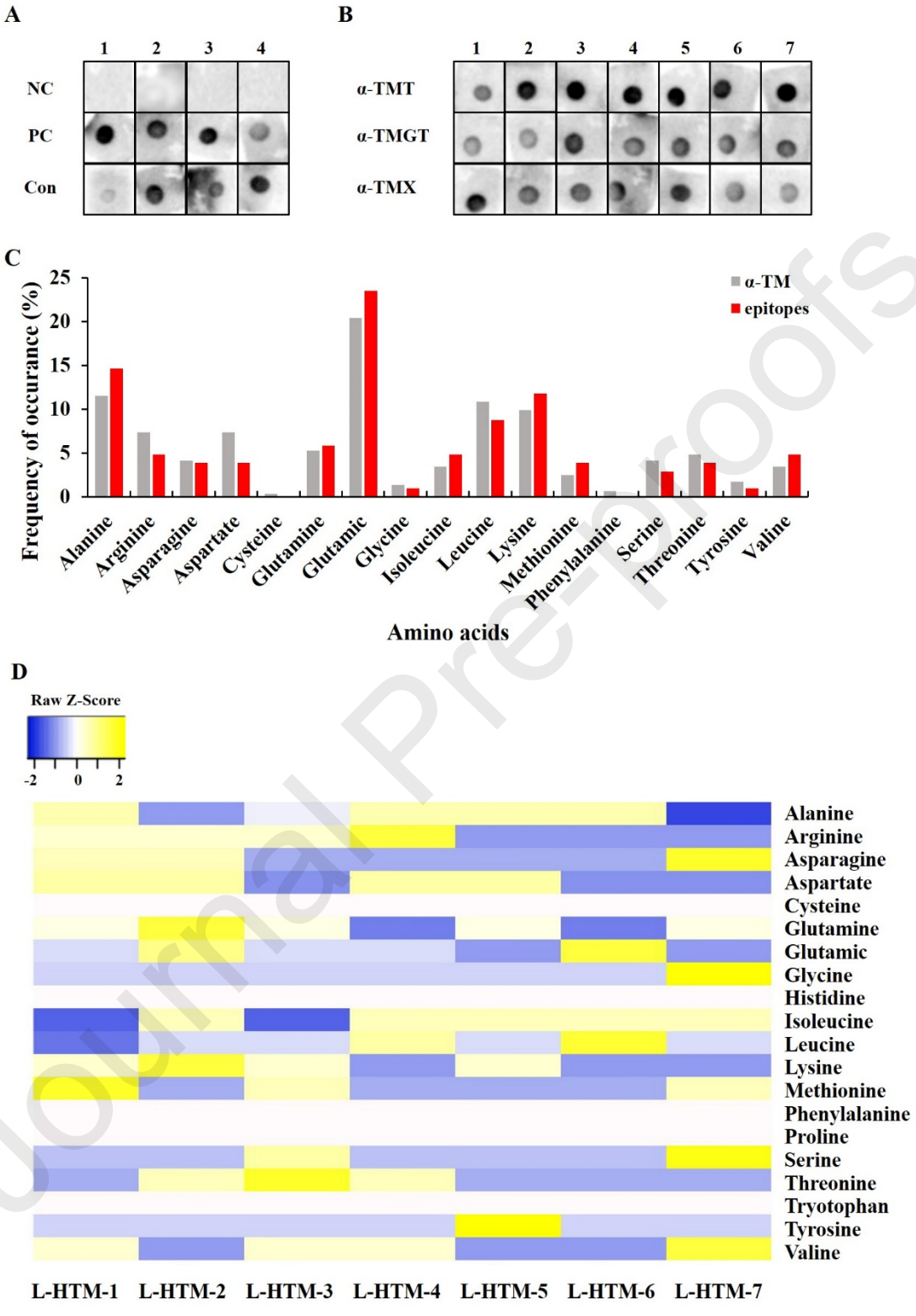

635

636 **Figure 5**

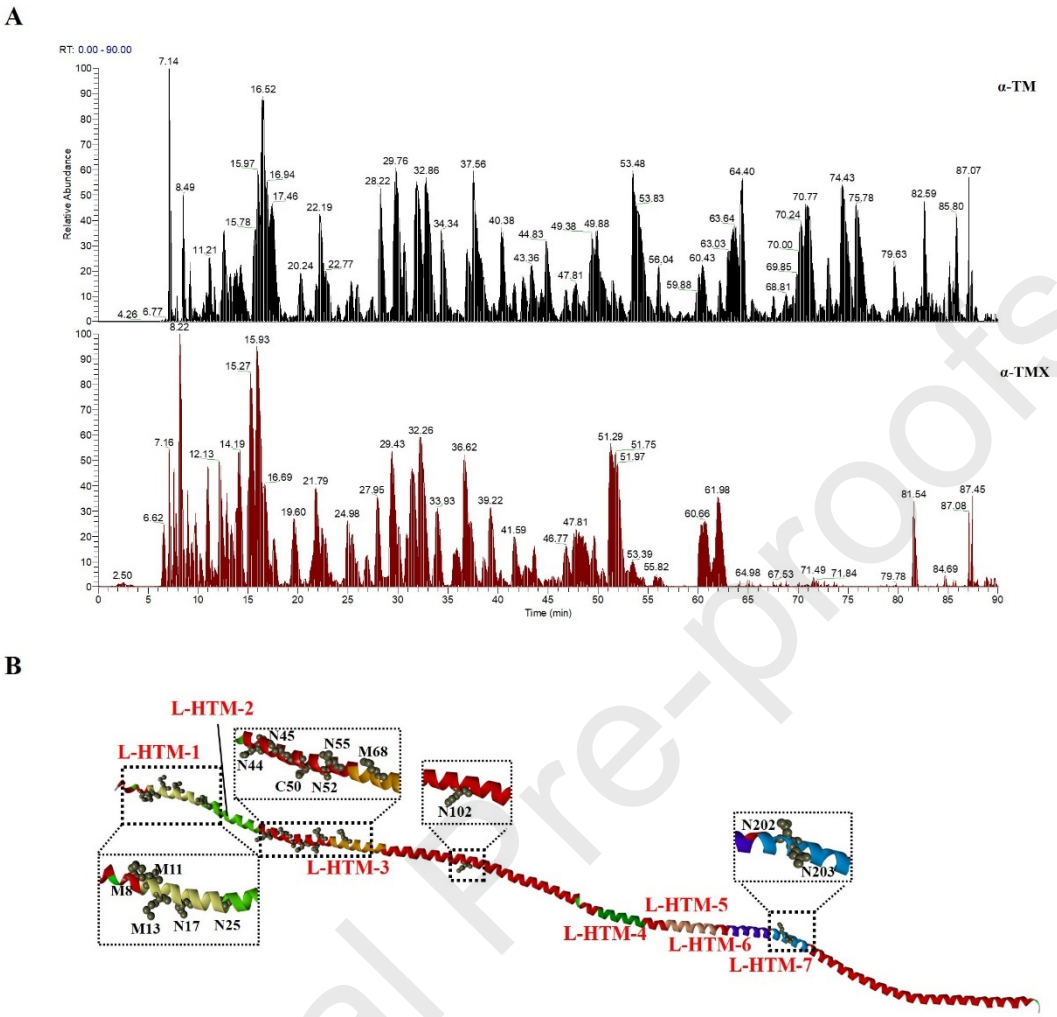

637

638 **Table of Contents Graphic**

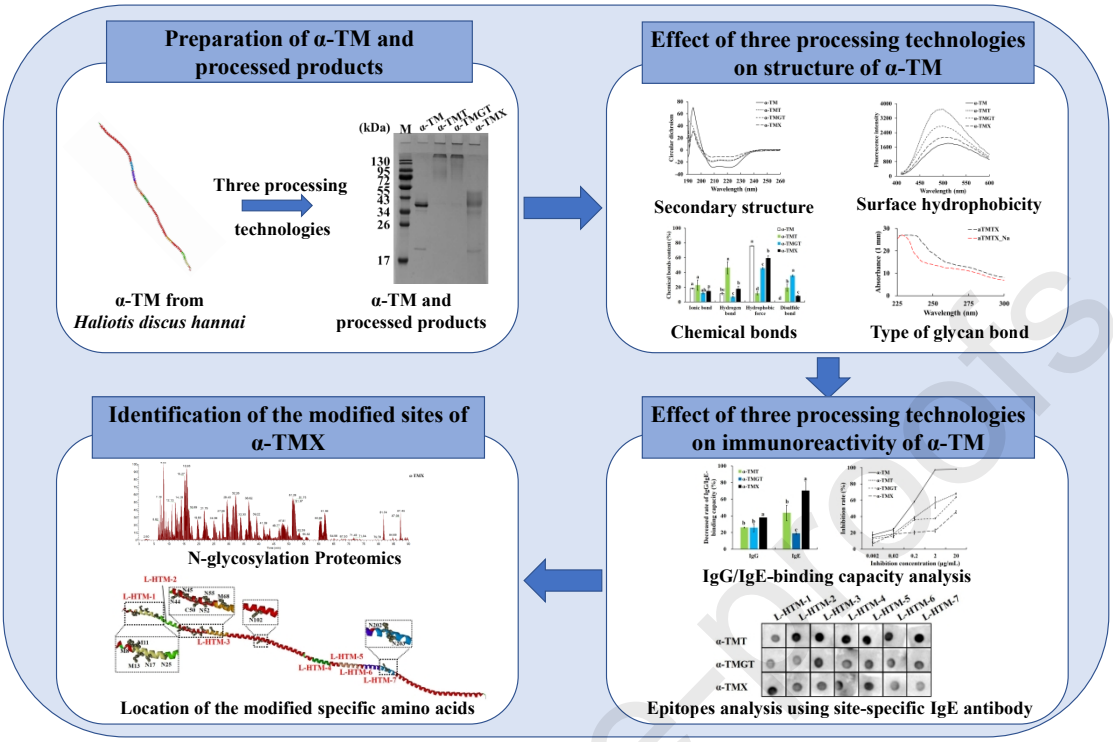

639
640

641 **Highlight**

642 1. Three processing technologies converted α-helix to β-sheet, β-turn, and random coil.

643 2. Glycation of TM by xylose reduced the immunoreactivity mostly.

644 3. Glycation of TM could modify two epitopes by three N-glycated sites.

645

646